STUDIA UBB PHYSICA, Vol. 60 (LX), 1, 2015, pp. 109-118
(RECOMMENDED CITATION)

Dedicated to Academician Professor Dr. Emil Burzo on His 80th Anniversary

CW EPR POWDER SIMULATIONS USING SPIRAL-TYPE GRIDS

C. CRĂCIUN[1*]

ABSTRACT. This paper compares two types of spiral grids from the point of view of their homogeneity and efficiency for CW EPR powder simulations. One grid is well-known in the EPR context and has a parameter-free analytical expression. The other grid has been defined for minimizing the potential energy of charged particles on the unit sphere and has an adjustable shape. The quality of EPR simulations produced by these spiral grids is analysed for a spin system S = 1/2, with different symmetry of the gyromagnetic matrix.

Keywords: *CW EPR, simulation, spiral grid*

INTRODUCTION

CW EPR powder spectra are calculated as a sum over the spectral contribution of all single-crystals composing the powder sample [1]. The single-crystals' orientations in the laboratory frame may be modelled using a spherical grid. The quality of EPR simulations depends on the orientational grid's type and size. Higher dimensional grids yield better simulated spectra, but they are time expensive for powder EPR simulations. Therefore, the grids with good EPR behaviour even at low size are preferred.

Different grids have been previously used for simulation of magnetic resonance spectra [1-13]. This paper analyses the homogeneity characteristics and the EPR behaviour of two spiral-type grids. The first spiral grid (MW) was proposed by Mombourquette and Weil in the context of EPR simulations [7]. This grid has a C_i symmetry [10], a high convergence rate in simulations [1], and a high homogeneity degree [10]. The second spiral grid (RSZ), known as the "generalised spiral", was proposed by Rakhmanov, Saff, and Zhou [14]. This grid was defined for minimizing the energy of a set of charged

[1] *Babeş-Bolyai University, Faculty of Physics, 1 Kogălniceanu str., 400084 Cluj-Napoca, Romania*
* *Corresponding author e-mail: cora.craciun@phys.ubbcluj.ro*

particles on the unit sphere, which interact through the logarithmic potential $V(r) = \log(1/r)$ [14]. The shape of the RSZ grid may be adjusted by means of a parameter in the grid's analytical expression. To the author's knowledge, the RSZ grid has not been previously used for EPR simulations.

This paper is structured as follows. Next section presents theoretical details about the two spiral grids and about CW EPR powder simulations. The grids' homogeneity degree and their EPR efficiency are compared in the Results and discussion section. The final section summarizes current work.

THEORETICAL AND COMPUTATIONAL DETAILS

1. The MW spiral grid

The MW grid (Fig. 1 f) consists in a single spiral which connects the poles of the unit sphere or an equator point and a pole [7]. At its proposal, the MW grid was generated with an optimization procedure, which ensured that the consecutive grid points on the spiral were equally-spaced [7]. Later, the grid was generated analytically and has the following expressions in spherical coordinates, on the full unit sphere [1,10]:

$$\theta_k = \arccos(h_k), \quad \phi_k = \Delta \arcsin(h_k), \tag{1}$$

$$\Delta = \sqrt{\pi(N-1)}, \quad h_k = \frac{2k}{N-1} - 1, \quad 0 \le k \le N-1.$$

Unlike the RSZ spiral grid, the MW grid has a fixed shape, at a given grid size *N*.

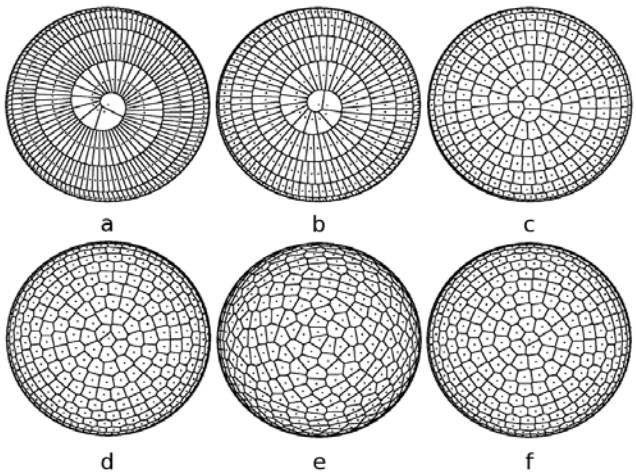

Fig. 1. The upper hemisphere of the MW spiral grid (f) and of the RSZ spiral grids with the following parameter *C*: (a) 1.2, (b) 1.6, (c) 2.6, (d) 3.4, and (e) 4.6. All grids have 578 points on the full unit sphere.

2. The RSZ spiral grid

The RSZ spiral grid in spherical coordinates is [14]

$$\theta_k = \arccos(h_k), \quad h_k = \frac{2(k-1)}{N-1} - 1, \quad 1 \le k \le N, \tag{2}$$
$$\phi_k = \left(\phi_{k-1} + C / \sqrt{N(1-h_k^2)}\right) (\mathrm{mod}\ 2\pi), \quad 2 \le k \le N-1, \quad \phi_1 = \phi_N = 0,$$

where N is the grid size, C is a parameter, and *mod* stands for the modulo operation. The best packing of the grid points on the unit sphere (the Tammes problem) was obtained with the parameter value $C = \left(8\pi / \sqrt{3}\right)^{1/2} \approx 3.809$ [15,16]. In the energy minimization context, however, the optimal value $C = 3.6$ was obtained by experimentation [14,16]. In this paper, the C parameter is varied between 1.0 and 4.8 with step 0.2, to obtain different RSZ grids for EPR simulations (Fig. 1 a-e).

The Voronoi diagrams of the spiral grids presented in Fig. 1 have been computed with the STRIPACK package (R.J. Renka) [17], in the implementation available at [18].

3. CW EPR powder simulations

CW EPR powder spectra for the spiral grids are compared for a spin system S = 1/2, characterised by electron Zeeman interaction with the static magnetic field. For this spin system, the simulated powder spectra have the following analytical form [19]:

$$S(B) \approx \sum_{k=1}^{N} w_k I_k F[B - B_0(\Omega_k), \Gamma] = \sum_{k=1}^{N} C_B w_k \frac{\langle g_1^2(\Omega_k) \rangle}{g(\Omega_k)} F[B - B_0(\Omega_k), \Gamma], \tag{3}$$

where $\Omega_k = (\theta_k, \phi_k)$ is the orientation of the static magnetic field in the molecular frame of the gyromagnetic matrix **g**, I_k is the linear spectral intensity at orientation Ω_k, $F[B - B_0(\Omega_k), \Gamma]$ is the line shape absorption function, centred at the resonance magnetic field B_0 and having the peak-to-peak line width Γ in the first derivative, w_k is the weighting factor, C_B is a constant, $g(\Omega_k)$ is the effective gyromagnetic value, and $\langle g_1^2(\Omega_k) \rangle$ is [19]:

$$\begin{aligned} \langle g_1^2(\Omega_k) \rangle = \big(g_x^2 g_y^2 (\sin\theta_k)^2 + g_y^2 g_z^2 \left[(\sin\phi_k)^2 + (\cos\theta_k \cos\phi_k)^2\right] + \\ + g_x^2 g_z^2 \left[(\cos\phi_k)^2 + (\cos\theta_k \sin\phi_k)^2\right]\big) / 2g^2(\Omega_k), \end{aligned} \tag{4}$$

with g_x, g_y, and g_z the principal values of the **g** matrix.

RESULTS AND DISCUSSION

1. The spiral grids' homogeneity

The weighting factor w_k in the CW EPR powder spectrum (formula 3) may be approximated with the area of the Voronoi cell corresponding to the k^{th} grid point. Therefore, the relative standard deviation of the m distribution of the Voronoi cells' areas A_k, for $1 \leq k \leq N$, has been chosen for comparing the grids' homogeneity [10]:

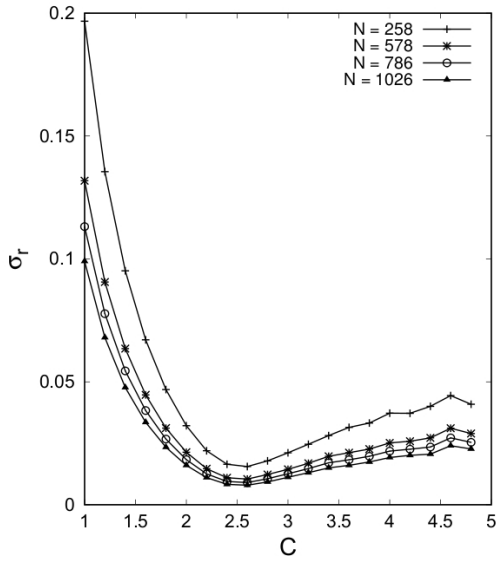

Fig. 2. Dependence of the σ_r homogeneity metric on the RSZ grid's parameter *C*, for different grid sizes *N*.

Table 1. The σ_r homogeneity metric for the RSZ (*C* = 2.6 and *C* = 3.4) and MW spiral grids, at different grid sizes *N*

N	σ_r (RSZ, *C* = 2.6)	σ_r (RSZ, *C* = 3.4)	σ_r (MW)
258	0.016	0.028	0.030
578	0.011	0.020	0.020
786	0.009	0.017	0.017
1026	0.008	0.015	0.015

$$\sigma_r = \sqrt{\frac{N}{16\pi^2}\sum_{k=1}^{N} A_k^2 - 1} \tag{5}$$

Table 2. Principal values of the **g** matrix used in EPR simulations. The symmetry of the **g** matrix (I - isotropic, A - axial, R - rhombic) is indicated in parenthesis in each case.

No.	g_x, g_y, g_z	No.	g_x, g_y, g_z	No.	g_x, g_y, g_z
1	2.0, 2.0, 2.0 (I)	10	2.1, 2.0, 2.0 (A)	19	2.2, 2.0, 2.0 (A)
2	2.0, 2.0, 2.1 (A)	11	2.1, 2.0, 2.1 (A)	20	2.2, 2.0, 2.1 (R)
3	2.0, 2.0, 2.2 (A)	12	2.1, 2.0, 2.2 (R)	21	2.2, 2.0, 2.2 (A)
4	2.0, 2.1, 2.0 (A)	13	2.1, 2.1, 2.0 (A)	22	2.2, 2.1, 2.0 (R)
5	2.0, 2.1, 2.1 (A)	14	2.1, 2.1, 2.1 (I)	23	2.2, 2.1, 2.1 (A)
6	2.0, 2.1, 2.2 (R)	15	2.1, 2.1, 2.2 (A)	24	2.2, 2.1, 2.2 (A)
7	2.0, 2.2, 2.0 (A)	16	2.1, 2.2, 2.0 (R)	25	2.2, 2.2, 2.0 (A)
8	2.0, 2.2, 2.1 (R)	17	2.1, 2.2, 2.1 (A)	26	2.2, 2.2, 2.1 (A)
9	2.0, 2.2, 2.2 (A)	18	2.1, 2.2, 2.2 (A)	27	2.2, 2.2, 2.2 (I)

The grids with smaller σ_r values are more homogeneous [10]. In case of RSZ spiral grids, the σ_r homogeneity metric presents a minimum when the grids' parameter *C* is about 2.6 (Fig. 2). At the same grid size, the RSZ grid has similar homogeneity with the MW grid when its parameter is $C \approx 3.4$ (Table 1). This *C* value is close to the 3.6 value determined from energy minimization considerations [16].

2. Simulated CW EPR powder spectra

Simulated spectra for the spiral grids with 578 points on the full unit sphere are compared with those of the MW grid with 9606 points, chosen as reference. The spin system considered is S = 1/2 and its **g** matrix is isotropic, axial, or rhombic (Table 2). The axial **g** matrices used in simulations have the x, y, or z orthogonal axis. The spiral grids given in formulas (1) and (2) are built around the z axis of the reference system. This z axis will be called in the following the main axis of the spiral grids.

Four simulation cases, two for axial and two for rhombic **g** matrices (Fig. 3), are discussed in the following. In Fig. 4 are given difference spectra obtained by subtracting the reference spectra, $S_0(B)$ (Fig. 3 g), from the spiral grids' spectra, $S(B)$ (Fig. 3 a-f):

$$d(B_j) = S(B_j) - S_0(B_j), \quad 1 \le j \le M, \tag{6}$$

where B_j are the equally-spaced magnetic fields at which the spectral intensity has been calculated. In the four simulation cases considered, the RSZ grid with *C* = 1.6 generates low-noise simulated spectra (Fig. 3 b), but there is a residual contribution along the g_z direction in its difference spectra (Fig. 4 b).

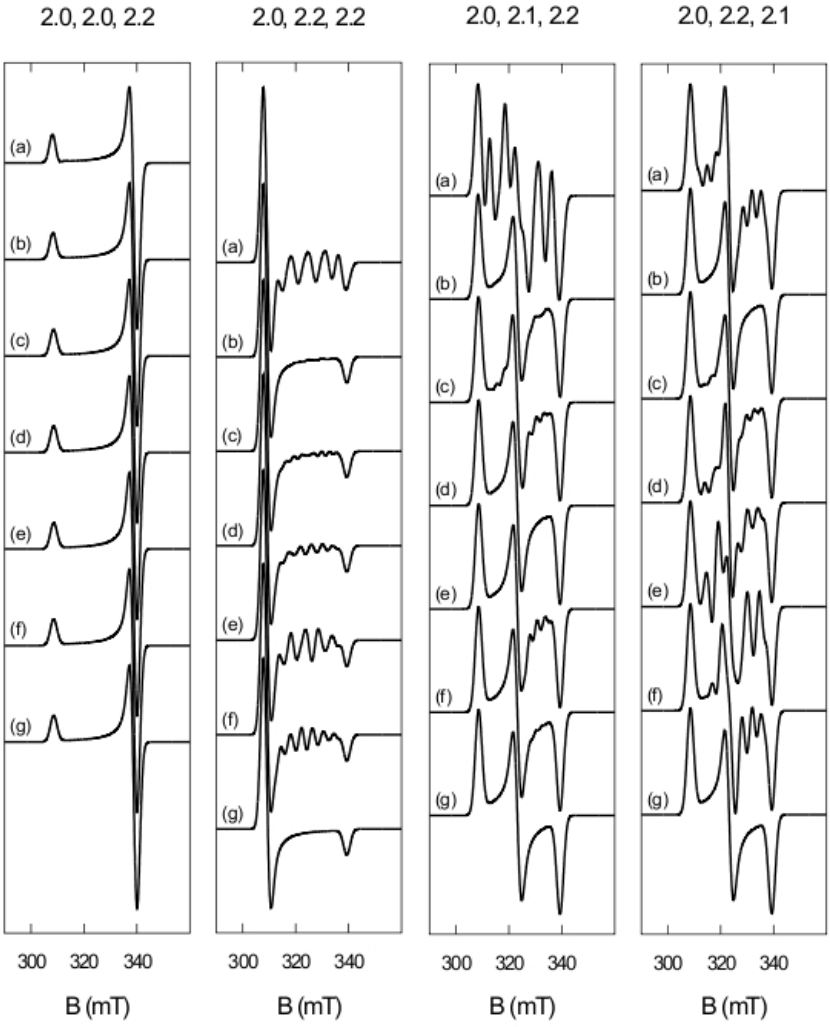

Fig. 3. Simulated CW EPR powder spectra (a-e) for the RSZ spiral grids with 578 points and the following *C* parameter: (a) 1.2, (b) 1.6, (c) 2.6, (d) 3.4, and (e) 4.6, (f) for the MW spiral grid with 578 points, and (g) for the reference MW grid with 9606 points. Principal values of the **g** matrix, g_x, g_y, and g_z, are indicated above each figure. Simulation parameters: microwave frequency ν = 9.5 GHz, full width at half maximum of the Gaussian line shape of 3 mT.

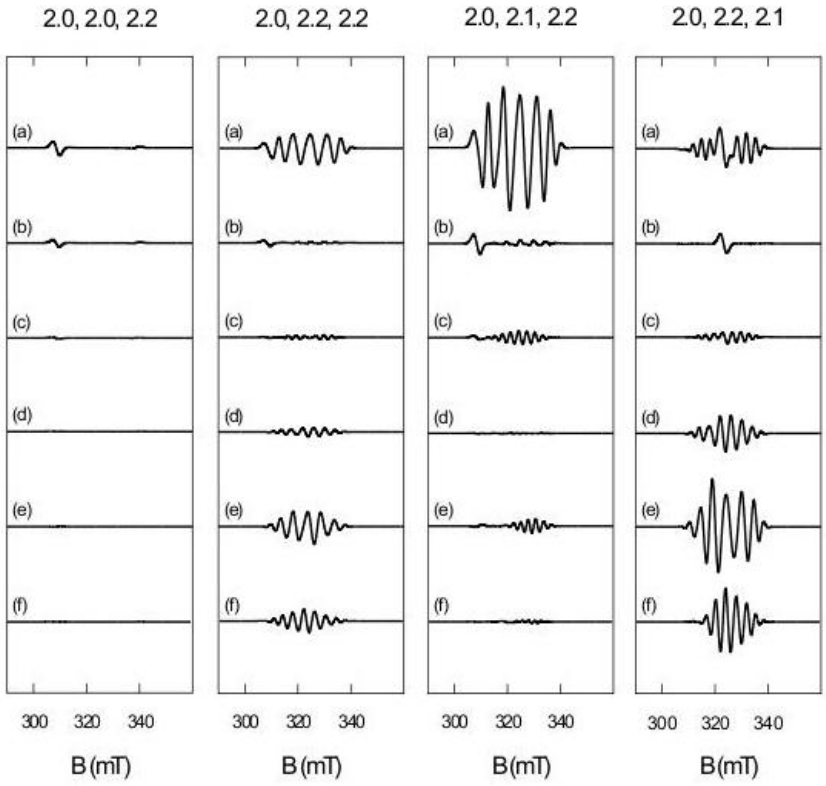

Fig. 4. Difference between the simulated spectra of the spiral grids with 578 points (Fig. 3 a-f) and the corresponding simulated spectra of the MW grid with 9606 points (Fig. 3 g), for the same **g** matrix.

i. $g_x = g_y = 2.0$, $g_z = 2.2$: For all values of the *C* parameter, the RSZ grids generate low-noise simulated spectra. The MW spiral grid (Fig. 3 f) and the RSZ grids with $C = 3.4$ and $C = 4.6$ (Fig. 3 d,e) have nearly the same simulated spectra as the reference grid (Fig. 3 g). This behaviour may be explained by two reasons: (1) the RSZ grids' high homogeneity degree (small σ_r values) for the two *C* values (Fig. 2) and (2) the coincidence between the RSZ grids' main axis and the **g** matrix axial axis.
ii. $g_x = 2.0$, $g_y = g_z = 2.2$: In this axial case, the grids' main axis (z) and the **g** matrix axial axis (x) do not coincide. The RSZ grids with $C = 1.6$, 2.6, and 3.4 (Fig. 3 and Fig. 4 b-d) have close EPR behaviour to the reference grid. One reason may be the high homogeneity degree of these RSZ grids (Fig. 2). However, the RSZ grid with $C = 4.6$ and the MW grid with 578 points are also homogeneous, but their simulated spectra (Fig. 3 e,f) are quite noisy.

iii. $g_x = 2.0$, $g_y = 2.1$, $g_z = 2.2$: For this rhombic case, the RSZ grid with $C = 3.4$ (Fig. 3 d) and the MW grid (Fig. 3 f) are the closest in EPR simulations to the reference grid (Fig. 3 g). The RSZ grid with $C = 1.2$ generates a very noisy EPR spectrum (Fig. 3 a) and it also has a low homogeneity degree (Fig. 2).

iv. $g_x = 2.0$, $g_y = 2.2$, $g_z = 2.1$: The spiral grids' difference spectra with respect to the reference spectrum (Fig. 4) resemble those from case (ii) discussed above. However, now the residual contribution in difference spectra is higher for the MW grid (Fig. 4 f) and for the RSZ grids with $C = 3.4$ and $C = 4.6$ (Fig. 4 d,e) than in the (ii) case. The ordering relation $g_y > g_z$ may be a possible reason.

As has been emphasised in reference [1], the MW spiral grid is more efficient in EPR simulations when its principal axes coincide with those of the dominant anisotropic interaction of the spin system. This is also true for the RSZ grids. If an RSZ grid built around the z axis of the reference system yields a noisy simulated EPR spectrum, then the grid built around the x or y axes may enhance the spectrum's quality. For example, the axial cases (9) and (25) in Table 2 have the same principal values of the

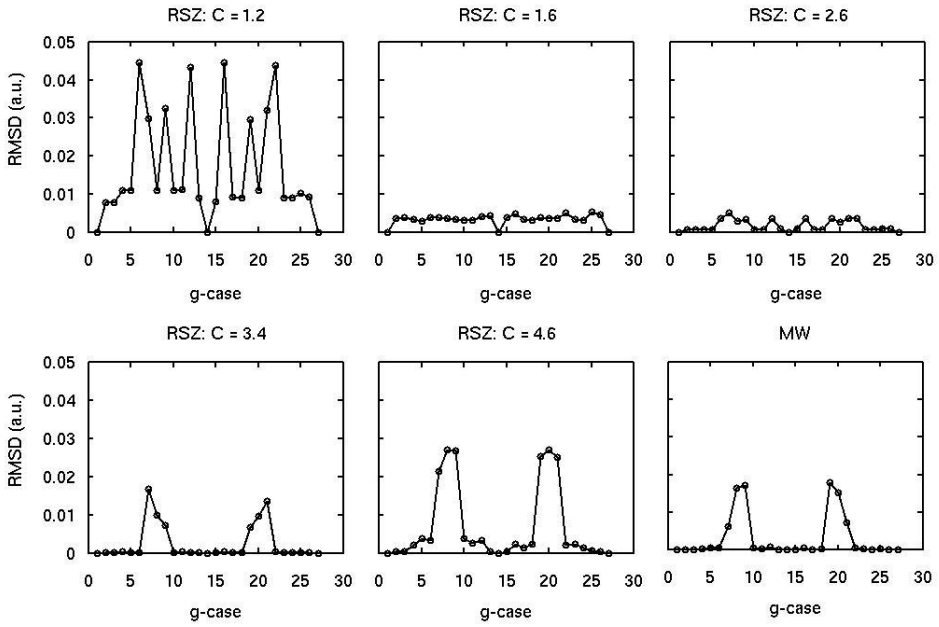

Fig. 5. The *RMSD* metric for the set of g-cases given in Table 2. The first five figures belong to the RSZ grids, with indicated *C* parameter, and the last figure belongs to the MW grid.

g matrix, but the g_x and g_z values are swapped. If the RSZ grid with C = 3.4 is built around the z axis, then the simulated spectrum in case (9) is noisy and that in case (25) is noise-free. Thus, using in case (9) an RSZ grid with the main axis x will produce a noise-free spectrum. A similar situation occurs in cases (8) (noisy) and (22) (noise-free), for the same RSZ grid with C = 3.4 and the main axis z.

The root-mean-square deviation (*RMSD*) was calculated between the simulated spectra of the spiral grids (578 points) and the corresponding simulated spectra of the reference MW grid (9606 points), for the g-cases given in Table 2. According to the *RMSD* metric, the simulated spectra for the RSZ grid with C = 1.2 differ the most from those of the reference grid in the rhombic g-cases (6), (12), (16), and (22), and in the axial g-cases (7), (9), (19), and (21) (Fig. 5, Table 2). For the RSZ grids with C = 1.6 and C = 2.6, *RMSD* is relatively small for all g-cases. The RSZ grids with C = 3.4 and C = 4.6 differ the most from the reference grid in the following g-cases: (7), (8), and (9), with maximal g_y value, and (19), (20), and (21), with maximal g_x value. The MW grid and the RSZ grid with C = 3.4 have close EPR behaviour for all **g** matrices considered.

CONCLUSIONS

This paper has compared the homogeneity degree and the behaviour in CW EPR powder simulations of two spiral-type grids: the grid proposed by Mombourquette and Weil (MW) and that proposed by Rakhmanov, Saff, and Zhou (RSZ). The RSZ spiral grid was generated in different variants, by means of an adjustable parameter C appearing in its analytical expression. The RSZ grid with C = 3.4 has similar characteristics with the MW grid; the RSZ grid with C = 2.6 is the most homogeneous concerning the distribution of its Voronoi cells' area; and the grids with C = 1.6, 2.6, and 3.4 generate relatively low-noise CW EPR powder spectra, for different symmetries of the gyromagnetic matrix.

REFERENCES

1. A. Ponti, *J. Magn. Reson.*, 138, 288 (1999).
2. M.J. Nilges, Ph.D. Thesis, University of Illinois, Urbana, Illinois, 1979.
3. S. Galindo, L. Gonzáles-Tovany, *J. Magn. Reson.*, 44, 250 (1981).
4. D.W. Alderman, M.S. Solum, D.M. Grant, *J. Chem. Phys.*, 84, 3717 (1986).
5. M.C.M. Gribnau, J.L.C. van Tits, E.J. Reijerse, *J. Magn. Reson.*, 90, 474 (1990).
6. A. Kreiter, J. Hüttermann, *J. Magn. Reson.*, 93, 12 (1991).
7. M.J. Mombourquette, J.A. Weil, *J. Magn. Reson.*, 99, 37 (1992).
8. D. Wang, G.R. Hanson, *J. Magn. Reson. A*, 117, 1 (1995).

9. M. Bak, N.C. Nielsen, *J. Magn. Reson.*, 125, 181 (1997).
10. S. Stoll, Ph.D. Thesis, ETH Zurich, Switzerland, 2003.
11. S. Stoll, A. Schweiger, *J. Magn. Reson.*, 178, 42 (2006).
12. C. Crăciun, *Appl. Magn. Reson.*, 38, 279 (2010).
13. C. Crăciun, *J. Magn. Reson.*, 245, 63 (2014).
14. E.A. Rakhmanov, E.B. Saff, Y.M. Zhou, *Math. Res. Letters*, 1, 647 (1994).
15. W. Habicht, B.L. van der Waerden, *Math. Ann.*, 123, 223 (1951).
16. E.B. Saff, A.B.J. Kuijlaars, *Math. Intell.*, 19, 5 (1997).
17. R.J. Renka, *ACM Trans. Math. Softw.*, 23, 416 (1997).
18. http://people.sc.fsu.edu/~jburkardt/f_src/f_src.html.
19. J.R. Pilbrow, "Transition Ion Electron Paramagnetic Resonance", Clarendon Press, Oxford, **1990**, pp. 222-229.